# Chapter 1
# Numerical simulation examples of a large-scale model

In this Chapter, we apply the fundamentals explained so far to perform numerical simulations of a standard large-scale model called the IEEE 68-bus system model. The structure of this chapter is as follows. First, in Section 1, we organize the numerical data of transmission lines, loads, and generators in the IEEE 68-bus system model. Next, in Section 2, we analyze the effect of automatic generation control on load fluctuations. Specifically, we analyze the changes in generator and bus variables when the load impedance changes gradually over a few hours. Finally, in Section 3, we analyze the transient stability of the system with respect to bus grounding. In particular, we demonstrate that incorporating system stabilizing devices independently designed for each generator based on retrofit control theory can significantly improve system stability.

## 1 Power system model under consideration

### 1.1 IEEE68 bus system model

In this section, we present numerical simulation results using the IEEE68 bus power system model (Figure 1). This model consists of 68 buses, with generators connected to 16 buses and loads connected to 35 buses. The ”Area 1” in Figure 1 represents the power system in the northeastern United States, while ”Area 2” represents the power system in the state of New York. In addition, Areas 3 to 5 represent the power systems around New York State, each represented by one set of generators and loads.

The transmission lines are modeled considering the ground capacitance as explained in Section **??**. The constants of each transmission line are set to the values shown in Table 1. The first column shows the bus numbers at both ends of the transmission line, and the second, third, and fourth columns show the resistance, reactance, and ground capacitance values of the transmission line, respectively. These are standard values shown in [**?**, Appendix A]. Furthermore, we use the salient-

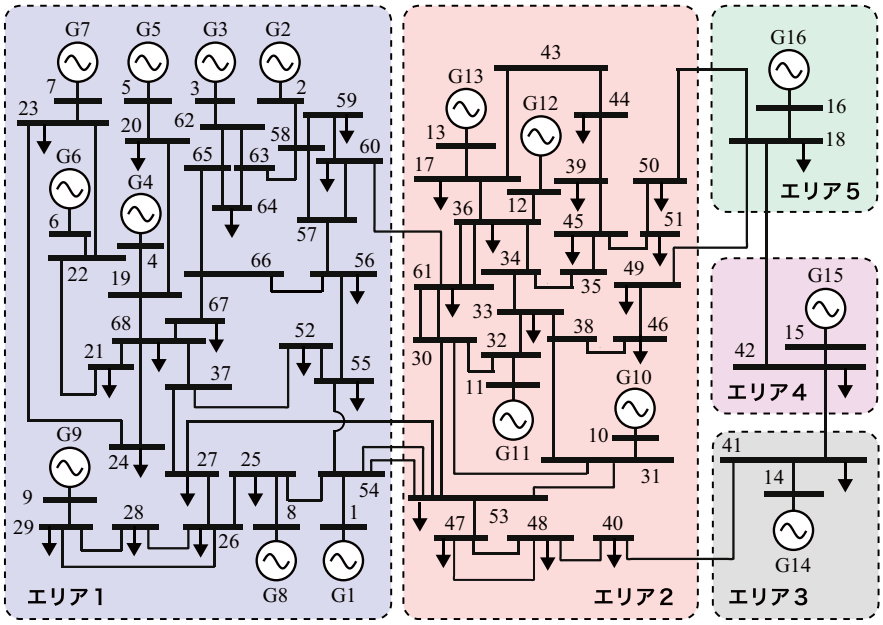


**Fig. 1 IEEE68 bus system model**

pole generator model explained in Section **??** for the generators. The constants for each generator are set to the values shown in Table 2, which are also shown in the aforementioned literature.

## 1.2 Data sheet for power flow calculation

The data sheets for the generator buses used in power flow calculations are shown in Table 3. Similarly, the data sheet for the load buses is shown in Table 4. These values are also cited from [**?**, Appendix A].

## 1.3 Load model

The constant impedance load model described in Section **??** is adopted for the load model. The impedance values of the loads determined from the power flow calculation results for the data sheets in Table 3 and Table 4 are shown in Table 5. Note that bus 16 is set as the slack bus, and the value of $P_{16}^{\star}$ is calculated as 33.68.

# 2 Frequency stability analysis for load fluctuations

## 2.1 Load fluctuation settings

In this section, we observe the time response of the angular frequency deviation when the impedance values of the loads are changed. The impedance values of the loads are increased linearly by 10% per hour based on the values in Table 5. That is, the impedance of each load is set as:

$$z_{\mathrm{load}i}(t) = \left(1 + \tfrac{1}{36000}t\right)(r_{\mathrm{load}i} + \boldsymbol{j}x_{\mathrm{load}i}) \tag{1}$$

where $t$ is the time in [s].

## 2.2 When the machine input and field input of the generator are constant

Consider the case where both the mechanical and excitation inputs to the generator, which are external inputs, are constant. From the steady-state power flow solution given in the data sheets of Table 3 and Table 4, the time response of the frequency deviation for all generators is shown in Figure 2(a) when the impedance of the load changes according to Equation 1. In this case, since the load disturbance causes an imbalance in supply and demand, the frequency deviation does not converge to zero. Moreover, due to the increase in power consumption as the impedance of the load increases, the frequency deviation initially increases in the negative direction for about 7 seconds, and then diverges in the positive direction as the power system model becomes unstable.

## 2.3 Case where the Mechanical Input is Constant

Consider the case where an automatic voltage regulator that controls the excitation input of the generator and a power system stabilizer are installed in all generators. The automatic voltage regulator is set to the IEEE ST1 model described in Section **??**. Specifically, for all generator buses $i$, it is set to:

$$\begin{cases} 0.015\dot{V}_{\mathrm{tr}i} = -V_{\mathrm{tr}i} + |\boldsymbol{V}_i| \\ \quad V_{\mathrm{field}i} = 20(V^{\star}_{\mathrm{ref}i} + V_{\mathrm{pss}i} - V_{\mathrm{tr}i}) \end{cases}$$

In addition, the power system stabilizer is set to the IEEE PSS1 model described in Section **??**. Specifically, for all generator buses $i$, it is set to:

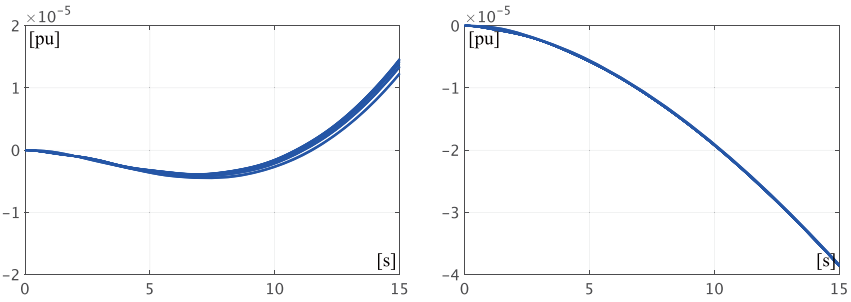


(a) Case where mechanical input and excitation input of the generator are constant

(b) Case where mechanical input of the generator is constant

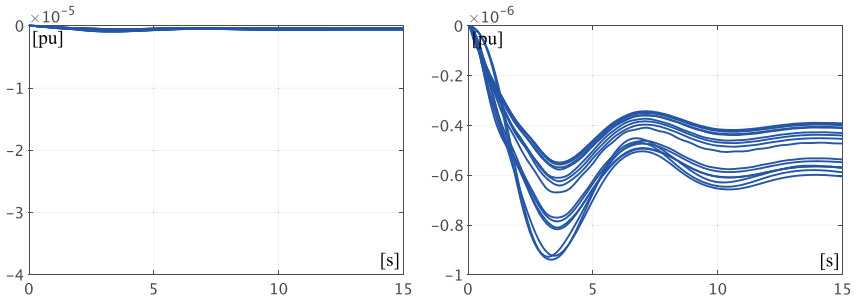


(c) Case where mechanical input of the generator is controlled

(d) Case where mechanical input of the generator is controlled (zoomed in)

**Fig. 2 Time response of angular frequency deviation to load variation**

$$\begin{cases} 1.4\dot{\xi}_{\mathrm{ws}i} = -\xi_{\mathrm{ws}i} + 9.5\Delta\omega_i \\ v_{\mathrm{ws}i} = 9.5\Delta\omega_i - \xi_{\mathrm{ws}i} \end{cases} \qquad \begin{cases} 0.033\dot{\xi}_i = -\xi_i + 0.79v_{\mathrm{ws}i} \\ V_{\mathrm{pss}i} = 4.67(v_{\mathrm{ws}i} - \xi_i) \end{cases}$$

The time response of the frequency deviation in this case is shown in Figure 2(b). Similar to Figure 2(a), it can be seen that due to load fluctuations, the supply-demand balance is not satisfied, and the frequency deviation does not become zero. Note that the mechanical input of the generator is also set to be constant for all generators, as described in Section 2.2.

## 2.4 Case where machine input is controlled by an automatic generation controller

Consider incorporating an automatic generator control to control the mechanical input of a generator. Here, for each area in Figure 1, we will incorporate the broadcast-type PI controller explained in Section **??**. Specifically, let $\mathcal{I}_{\mathrm{G}}^{(l)}$ denote the index set of generator buses in area $l$. Then, for the automatic generator control in area $l$, we set:

$$\begin{cases} \dot{\xi}^{(l)} = \Delta\omega_{\mathrm{ave}}^{(l)} \\ P_{\mathrm{mech}i} = P_i^\star - \frac{P_i^\star}{P_{\mathrm{ave}}^\star}\left(100\Delta\omega_{\mathrm{ave}}^{(l)} + 500\xi^{(l)}\right), \qquad i \in \mathcal{I}_{\mathrm{G}}^{(l)} \end{cases}$$

where we define the average of the deviation of angular frequency and the average of the active power in steady-state for the generators in area $l$ as follows:

$$\Delta\omega_{\mathrm{ave}}^{(l)}(t) := \frac{1}{|\mathcal{I}_{\mathrm{G}}^{(l)}|}\sum_{i\in\mathcal{I}_{\mathrm{G}}^{(l)}}\Delta\omega_i(t), \qquad P_{\mathrm{ave}}^\star := \frac{1}{16}\sum_{i=1}^{16}P_i^\star$$

It is assumed that each generator is equipped with an automatic voltage regulator as explained in Section 2.3.

The time response of the frequency deviation in this case is shown in Figure 2(c). Note that Figure 2(d) is an enlarged version of the y-axis scale. As a result of the automatic generation control, it can be seen that the frequency deviation is maintained around 0. Although the impedance value of the load continues to change, the frequency deviation does not become exactly 0, but remains at a small value of about $-1 \times 10^{-6}$ [pu].

Next, the changes in generator variables and bus variables from the initial time to 3 hours later are shown in Figure 3. Figures 3(a)-(d) represent the changes in $E_i e^{\boldsymbol{j}\,\delta_i}$, $\boldsymbol{V}_i$, $\boldsymbol{I}_i$, and $P_i + \boldsymbol{j}Q_i$, respectively, on a polar coordinate plane. The circle marks indicate the values at the initial time $t = 0$, and the square marks indicate the values at the final time $t = 10800$. The following can be observed from this figure:

- Figure 3(a):The internal voltage of all generators is maintained at around 0.7 to 1.5 [pu], and the rotor angle changes gradually in a clockwise direction.
- Figure 3(b):The absolute value of the bus voltage is maintained around 1 [pu], and its phase changes gradually in a clockwise direction like the rotor angle.
- Figure 3(c):The absolute value of the bus current increases as the consumption power increases with the increase in the impedance value of the load.
- Figure 3(d):As the impedance value of the load increases, the supplied active power and reactive power to the bus increase.

From these results, it can be seen that frequency stabilization is appropriately achieved by automatic generation control. In addition, for gradual load changes, it can be seen that the internal state of the generators changes gradually without oscillation, i.e., the entire power system is in a quasi-steady state.

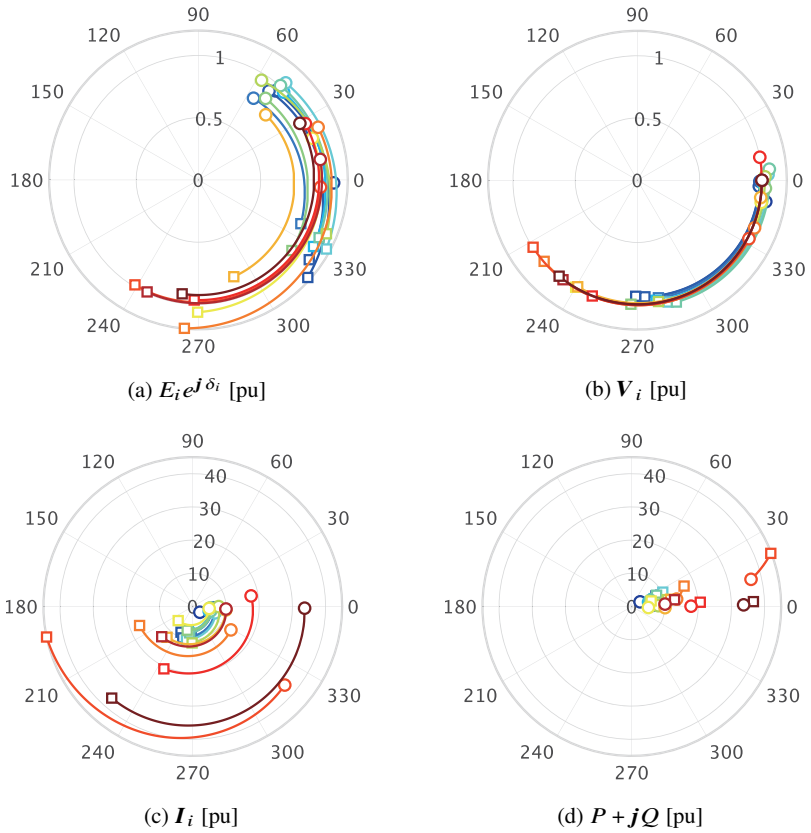


(a) $E_i e^{j\delta_i}$ [pu]

(b) $\boldsymbol{V}_i$ [pu]

(c) $\boldsymbol{I}_i$ [pu]

(d) $P + jQ$ [pu]

**Fig. 3 Changes in generator and bus variables due to load variations.**
(Circle: initial time, square: end time)

## 3 Transient stability analysis for bus ground faults

### 3.1 Setting of ground fault

In this section, we conduct a transient stability analysis of bus grounding. The transient stability of a power system is evaluated as follows: Let $\Delta\omega_i^{(k)}$ denote the angular frequency deviation of generator $i$ at bus $k$ caused by a ground fault. Then, the sensitivity of the angular frequency deviation of the entire power system to the grounding of bus $k$ is evaluated by the $\mathcal{L}_2$-norm of $\Delta\omega^{(k)}$, where $\Delta\omega^{(k)}$ is a vector consisting of the angular frequency deviations $\Delta\omega_1^{(k)}, \ldots, \Delta\omega_{16}^{(k)}$ of all generators at bus $k$. Furthermore, we define the sets of $\|\Delta\omega^{(k)}\|_{\mathcal{L}2}$ for all generator buses and load buses, respectively, as

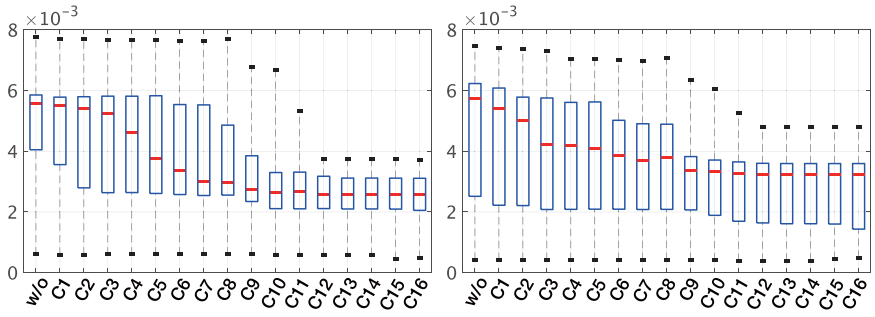


(a) $\mathcal{J}_{\mathrm{G}}$: Ground fault on generator buses (b) $\mathcal{J}_{\mathrm{L}}$: Ground fault on load buses

**Fig. 4 Evaluation of system stability with respect to bus ground fault**

$$\mathcal{J}_{\mathrm{G}} := \left\{ \|\Delta\omega^{(k)}\|_{\mathcal{L}_2} \right\}_{k\in\{1,\ldots,16\}}, \qquad \mathcal{J}_{\mathrm{L}} := \left\{ \|\Delta\omega^{(k)}\|_{\mathcal{L}_2} \right\}_{k\in\{17,\ldots,68\}}$$

Considering that a ground fault can occur at any bus, not just a specific bus, the transient stability of bus grounding can be evaluated by considering the smallness of the data sets $\mathcal{J}_{\mathrm{G}}$ and $\mathcal{J}_{\mathrm{L}}$ in an appropriate sense. In this section, we use the maximum value, minimum value, and quartiles of $\mathcal{J}_{\mathrm{G}}$ and $\mathcal{J}_{\mathrm{L}}$ shown in box plots to compare the transient stability, in order to visualize the size of the data dispersion. Note that the duration of the ground fault is set to 70 [ms] for all buses.

First, we analyze the transient stability when all generators are equipped with standard automatic voltage regulators and system stabilizers. The parameter settings are the same as in Section 2.3. The results of the obtained data sets $\mathcal{J}_{\mathrm{G}}$ and $\mathcal{J}_{\mathrm{L}}$ displayed as boxplots are shown in the first column of Figure 4. Figure 4(a) shows $\mathcal{J}_{\mathrm{G}}$ regarding the ground fault on the generator bus, and Figure 4(b) shows $\mathcal{J}_{\mathrm{L}}$ regarding the ground fault on the load bus. Subsequently, we evaluate the improvement of transient stability due to the addition of local controllers based on these values as a reference.

## 3.2 Effect of power system stabilizers bassed on retrofit control theory

We analyze the transient stability when power system stabilizers based on the retrofit control theory explained in Section **??** are incorporated into each generator. The retrofit controllers incorporated into each generator use the parameters of the approximate linear environment model identified from measurement data using the procedure described in Example **??**. In addition to the automatic voltage regulator, the model of the power system stabilizer is also used in the local linear subsystem

$G_i$. Furthermore, the controller that stabilizes each design model $G_i^+$ is designed based on the linear quadratic regulator design method explained in Section **??**.

In this case, we show the results of displaying the obtained data sets $\mathcal{J}_{\mathrm{G}}$ and $\mathcal{J}_{\mathrm{L}}$ as box-and-whisker plots in the second to seventeenth columns of Figure 4. The horizontal axis "C$i$" represents the case where retrofit controllers are incorporated into all generators from generator 1 to generator $i$. From these results, we can see that the transient stability gradually improves as the number of retrofit controllers incorporated increases.

**Table 1 Physical constants of transmission lines**

| $i$–$j$ | $r_{ij}$ | $x_{ij}$ | $c_{ij}$ |
|---|---|---|---|
| 1–54 | 0 | 0.0181 | 0 |
| 2–58 | 0 | 0.0250 | 0 |
| 3–62 | 0 | 0.0200 | 0 |
| 4–19 | 0.0007 | 0.0142 | 0 |
| 5–20 | 0.0009 | 0.0180 | 0 |
| 6–22 | 0 | 0.0143 | 0 |
| 7–23 | 0.0005 | 0.0272 | 0 |
| 8–25 | 0.0006 | 0.0232 | 0 |
| 9–29 | 0.0008 | 0.0156 | 0 |
| 10–31 | 0 | 0.0260 | 0 |
| 11–32 | 0 | 0.0130 | 0 |
| 12–36 | 0 | 0.0075 | 0 |
| 13–17 | 0 | 0.0033 | 0 |
| 14–41 | 0 | 0.0015 | 0 |
| 15–42 | 0 | 0.0015 | 0 |
| 16–18 | 0 | 0.0030 | 0 |
| 17–36 | 0.0005 | 0.0045 | 0.3200 |
| 17–43 | 0.0005 | 0.0276 | 0 |
| 18–42 | 0.0040 | 0.0600 | 2.2500 |
| 18–49 | 0.0076 | 0.1141 | 1.1600 |
| 19–20 | 0.0007 | 0.0138 | 0 |
| 19–68 | 0.0016 | 0.0195 | 0.3040 |
| 21–22 | 0.0008 | 0.0140 | 0.2565 |
| 21–68 | 0.0008 | 0.0135 | 0.2548 |
| 22–23 | 0.0006 | 0.0096 | 0.1846 |
| 23–24 | 0.0022 | 0.0350 | 0.3610 |
| 24–68 | 0.0003 | 0.0059 | 0.0680 |
| 25–26 | 0.0032 | 0.0323 | 0.5310 |
| 25–54 | 0.0070 | 0.0086 | 0.1460 |
| 26–27 | 0.0014 | 0.0147 | 0.2396 |
| 26–28 | 0.0043 | 0.0474 | 0.7802 |
| 26–29 | 0.0057 | 0.0625 | 1.0290 |
| 27–37 | 0.0013 | 0.0173 | 0.3216 |
| 27–53 | 0.0320 | 0.3200 | 0.4100 |
| 28–29 | 0.0014 | 0.0151 | 0.2490 |
| 30–31 | 0.0013 | 0.0187 | 0.3330 |
| 30–32 | 0.0024 | 0.0288 | 0.4880 |
| 30–53 | 0.0008 | 0.0074 | 0.4800 |
| 30–61 | 0.0019 | 0.0183 | 0.2900 |
| 30–61 | 0.0019 | 0.0183 | 0.2900 |
| 31–38 | 0.0011 | 0.0147 | 0.2470 |
| 31–53 | 0.0016 | 0.0163 | 0.2500 |
| 32–33 | 0.0008 | 0.0099 | 0.1680 |
| 33–34 | 0.0011 | 0.0157 | 0.2020 |
| 33–38 | 0.0036 | 0.0444 | 0.6930 |
| 34–35 | 0.0001 | 0.0074 | 0 |
| 34–36 | 0.0033 | 0.0111 | 1.4500 |
| 35–45 | 0.0007 | 0.0175 | 1.3900 |
| 36–61 | 0.0022 | 0.0196 | 0.3400 |
| 36–61 | 0.0022 | 0.0196 | 0.3400 |
| 37–52 | 0.0007 | 0.0082 | 0.1319 |
| 37–68 | 0.0007 | 0.0089 | 0.1342 |
| 38–46 | 0.0022 | 0.0284 | 0.4300 |
| 39–44 | 0 | 0.0411 | 0 |
| 39–45 | 0 | 0.0839 | 0 |
| 40–41 | 0.0060 | 0.0840 | 3.1500 |
| 40–48 | 0.0020 | 0.0220 | 1.2800 |
| 41–42 | 0.0040 | 0.0600 | 2.2500 |
| 43–44 | 0.0001 | 0.0011 | 0 |
| 44–45 | 0.0025 | 0.0730 | 0 |
| 45–51 | 0.0004 | 0.0105 | 0.7200 |
| 46–49 | 0.0018 | 0.0274 | 0.2700 |
| 47–48 | 0.0025 | 0.0268 | 0.4000 |
| 47–48 | 0.0025 | 0.0268 | 0.4000 |
| 47–53 | 0.0013 | 0.0188 | 1.3100 |
| 50–51 | 0.0009 | 0.0221 | 1.6200 |
| 52–55 | 0.0011 | 0.0133 | 0.2138 |
| 53–54 | 0.0035 | 0.0411 | 0.6987 |
| 54–55 | 0.0013 | 0.0151 | 0.2572 |
| 55–56 | 0.0013 | 0.0213 | 0.2214 |
| 56–57 | 0.0008 | 0.0128 | 0.1342 |
| 56–66 | 0.0008 | 0.0129 | 0.1382 |
| 57–58 | 0.0002 | 0.0026 | 0.0434 |
| 58–59 | 0.0006 | 0.0092 | 0.1130 |
| 57–60 | 0.0008 | 0.0112 | 0.1476 |
| 59–60 | 0.0004 | 0.0046 | 0.0780 |
| 60–61 | 0.0023 | 0.0363 | 0.3804 |
| 58–63 | 0.0007 | 0.0082 | 0.1389 |
| 62–63 | 0.0004 | 0.0043 | 0.0729 |
| 62–65 | 0.0004 | 0.0043 | 0.0729 |
| 63–64 | 0.0016 | 0.0435 | 0 |
| 64–65 | 0.0016 | 0.0435 | 0 |
| 65–66 | 0.0009 | 0.0101 | 0.1723 |
| 66–67 | 0.0018 | 0.0217 | 0.3660 |
| 67–68 | 0.0009 | 0.0094 | 0.1710 |

**Table 2 Physical constants of generators**

| $i$ | $M_i$ | $D_i$ | $\tau_i$ | $X_{\mathrm{d}i}$ | $X_{\mathrm{q}i}$ | $X'_{\mathrm{d}i}$ |
|---|---|---|---|---|---|---|
| 1 | 42.0 | 4.00 | 10.20 | 0.100 | 0.069 | 0.031 |
| 2 | 30.2 | 9.75 | 6.56 | 0.295 | 0.282 | 0.070 |
| 3 | 35.8 | 10.00 | 5.70 | 0.250 | 0.237 | 0.053 |
| 4 | 28.6 | 10.00 | 5.69 | 0.262 | 0.258 | 0.044 |
| 5 | 26.0 | 3.00 | 5.40 | 0.330 | 0.310 | 0.066 |
| 6 | 34.8 | 10.00 | 7.30 | 0.254 | 0.241 | 0.050 |
| 7 | 26.4 | 8.00 | 5.66 | 0.295 | 0.292 | 0.049 |
| 8 | 24.3 | 9.00 | 6.70 | 0.290 | 0.280 | 0.057 |
| 9 | 34.5 | 14.00 | 4.79 | 0.211 | 0.205 | 0.057 |
| 10 | 31.0 | 5.56 | 9.37 | 0.169 | 0.115 | 0.046 |
| 11 | 28.2 | 13.60 | 4.10 | 0.128 | 0.123 | 0.018 |
| 12 | 92.3 | 13.50 | 7.40 | 0.101 | 0.095 | 0.031 |
| 13 | 248.0 | 33.00 | 5.90 | 0.030 | 0.029 | 0.006 |
| 14 | 300.0 | 100.00 | 4.10 | 0.018 | 0.017 | 0.003 |
| 15 | 300.0 | 100.00 | 4.10 | 0.018 | 0.017 | 0.003 |
| 16 | 225.0 | 50.00 | 7.80 | 0.036 | 0.033 | 0.007 |

**Table 3 Datasheet for tidal current calculations (generator bus bar)**

| $i$ | $P_i^\star$ | $\lvert V_i^\star\rvert$ | $i$ | $P_i^\star$ | $\lvert V_i^\star\rvert$ | $i$ | $P_i^\star$ | $\lvert V_i^\star\rvert$ |
|---|---|---|---|---|---|---|---|---|
| 1 | 2.50 | 1.045 | 7 | 5.60 | 1.063 | 13 | 35.91 | 1.011 |
| 2 | 5.45 | 0.980 | 8 | 5.40 | 1.030 | 14 | 17.85 | 1.000 |
| 3 | 6.50 | 0.983 | 9 | 8.00 | 1.025 | 15 | 10.00 | 1.000 |
| 4 | 6.32 | 0.997 | 10 | 5.00 | 1.010 | 16 | 40.00 | 1.000 |
| 5 | 5.05 | 1.011 | 11 | 10.00 | 1.000 | | | |
| 6 | 7.00 | 1.050 | 12 | 13.50 | 1.016 | | | |

**Table 4 Datasheet used for tidal current calculations (load bus bar)**

| $i$ | $P_i^\star$ | $Q_i^\star$ | $i$ | $P_i^\star$ | $Q_i^\star$ | $i$ | $P_i^\star$ | $Q_i^\star$ |
|---|---|---|---|---|---|---|---|---|
| 17 | −60.00 | −3.00 | 35 | 0 | 0 | 53 | −2.52 | −1.19 |
| 18 | −24.70 | −1.23 | 36 | −1.02 | 0.19 | 54 | 0 | 0 |
| 19 | 0 | 0 | 37 | 0 | 0 | 55 | −3.22 | −0.02 |
| 20 | −6.80 | −1.03 | 38 | 0 | 0 | 56 | −2.00 | −0.74 |
| 21 | −2.74 | −1.15 | 39 | −2.67 | −0.13 | 57 | 0 | 0 |
| 22 | 0 | 0 | 40 | −0.65 | −0.24 | 58 | 0 | 0 |
| 23 | −2.48 | −0.85 | 41 | −10.00 | −2.50 | 59 | −2.34 | −0.84 |
| 24 | −3.09 | 0.92 | 42 | −11.50 | −2.50 | 60 | −2.09 | −0.71 |
| 25 | −2.24 | −0.47 | 43 | 0 | 0 | 61 | −1.04 | −1.25 |
| 26 | −1.39 | −0.17 | 44 | −2.68 | −0.05 | 62 | 0 | 0 |
| 27 | −2.81 | −0.76 | 45 | −2.08 | −0.21 | 63 | 0 | 0 |
| 28 | −2.06 | −0.28 | 46 | −1.51 | −0.29 | 64 | −0.09 | −0.88 |
| 29 | −2.84 | −0.27 | 47 | −2.03 | −0.33 | 65 | 0 | 0 |
| 30 | 0 | 0 | 48 | −2.41 | −0.02 | 66 | 0 | 0 |
| 31 | 0 | 0 | 49 | −1.64 | −0.29 | 67 | −3.20 | −1.53 |
| 32 | 0 | 0 | 50 | −1.00 | 1.47 | 68 | −3.29 | −0.32 |
| 33 | −1.12 | 0 | 51 | −3.37 | 1.22 | | | |
| 34 | 0 | 0 | 52 | −1.58 | −0.30 | | | |

**Table 5 Load impedance**

| $i$ | $r_{\mathrm{load}i}$ | $x_{\mathrm{load}i}$ | $i$ | $r_{\mathrm{load}i}$ | $x_{\mathrm{load}i}$ | $i$ | $r_{\mathrm{load}i}$ | $x_{\mathrm{load}i}$ |
|---|---|---|---|---|---|---|---|---|
| 17 | −60.00 | −3.00 | 35 | 0 | 0 | 53 | −2.52 | −1.19 |
| 18 | −24.70 | −1.23 | 36 | −1.02 | 0.19 | 54 | 0 | 0 |
| 19 | 0 | 0 | 37 | 0 | 0 | 55 | −3.22 | −0.02 |
| 20 | −6.80 | −1.03 | 38 | 0 | 0 | 56 | −2.00 | −0.74 |
| 21 | −2.74 | −1.15 | 39 | −2.67 | −0.13 | 57 | 0 | 0 |
| 22 | 0 | 0 | 40 | −0.65 | −0.24 | 58 | 0 | 0 |
| 23 | −2.48 | −0.85 | 41 | −10.00 | −2.50 | 59 | −2.34 | −0.84 |
| 24 | −3.09 | 0.92 | 42 | −11.50 | −2.50 | 60 | −2.09 | −0.71 |
| 25 | −2.24 | −0.47 | 43 | 0 | 0 | 61 | −1.04 | −1.25 |
| 26 | −1.39 | −0.17 | 44 | −2.68 | −0.05 | 62 | 0 | 0 |
| 27 | −2.81 | −0.76 | 45 | −2.08 | −0.21 | 63 | 0 | 0 |
| 28 | −2.06 | −0.28 | 46 | −1.51 | −0.29 | 64 | −0.09 | −0.88 |
| 29 | −2.84 | −0.27 | 47 | −2.03 | −0.33 | 65 | 0 | 0 |
| 30 | 0 | 0 | 48 | −2.41 | −0.02 | 66 | 0 | 0 |
| 31 | 0 | 0 | 49 | −1.64 | −0.29 | 67 | −3.20 | −1.53 |
| 32 | 0 | 0 | 50 | −1.00 | 1.47 | 68 | −3.29 | −0.32 |
| 33 | −1.12 | 0 | 51 | −3.37 | 1.22 | | | |
| 34 | 0 | 0 | 52 | −1.58 | −0.30 | | | |